

Process Waste Heat Recovery with a Supercritical Carnot Engine

Sarah Makuc¹, E. H. Chimowitz²

Abstract—We describe the optimization of a supercritical CO₂ Carnot engine aimed at utilizing waste heat from industrial processes. The approach is illustrated using data from a flow sheet for a toluene production chemical process [1], [2]. First, the maximum power that can be drawn from a stream carrying waste heat in the process is calculated. This heat is coupled with a supercritical working fluid Carnot engine and calculations are carried out to optimize the size and frequency of the engine. The impact of compression ratio, upper isotherm temperature, and engine pressure are considered. It is found that with a relatively small engine and frequency, on the order of 1.5 L and 50 Hz, having a moderate upper isotherm temperature and a compression ratio of 2, almost 1 million kWh of energy is recovered from a single waste stream, thereby reducing cooler loads, energy costs, and environmental emissions. The approach provides a novel computational adjunct for calculating the efficient potential recovery of waste heat in chemical process design.

I. INTRODUCTION

Efficient heat transfer is important in many areas of technology ranging from electrical power generation in coal, natural gas, and nuclear power plants, to refrigeration processes in industrial settings [3], [4], [5]. Power plants usually require the withdrawal of water from a freshwater supply reservoir for use as the coolant medium in condensers and/or recirculating wet-cooling towers where residual heat from the turbine exhaust stream is dissipated. This results in significant water loss through evaporation before being recycled to the process [6]. Additionally, water is often utilized in these processes as the working fluid. Therefore, in power plant systems, efficient waste heat recovery with working fluids other than water will lead to reduced water usage, which is a significant issue in many locations around the world [7]. For example, industrial values for condensing cooling water flows in typical 1000 MW coal and nuclear power plants are in the range of 300-1000 gpm/MW, which requires a large amount of water to be readily available. In the U.S., steam-electric power plants alone account for a high percentage of freshwater takeoff and consumption.

The theoretical thermodynamic efficiency of all of these processes depends upon a number of factors, foremost amongst is the Carnot efficiency, proportional to the temperature difference between heat input and rejection legs of the process [5]. Another important issue for reducing the size of heat transfer equipment in these systems is the magnitude of heat transfer coefficients available, especially in the cooling leg of the process. In supercritical fluids these coefficients are large, on the same order of magnitude of those found

in condensing steam systems[8], [9], [10], [11], [12], [13], [14], [15], [16].

In coal-fired plants the combustion temperature can be approximately 1500°C, while the rejection temperature is limited by ambient temperature of the cooling water reservoir. To increase the efficiency of power generation in these industrial processes, an additional step is often incorporated to recover waste heat from gas turbine exhausts, thereby generating additional steam to spin turbines that boost overall plant efficiency. These combined-cycle processes, however, usually recover heat from high temperature streams and are not suitable for capturing ‘waste’ heat available at lower temperatures where water would not work as the transfer fluid given its high boiling point. In such cases, the process has to be able accept heat at a relatively low temperature and reject it at an even lower one. Tijani presents data from the Energy Research Center of the Netherlands showing that in advanced economies, a large amount of waste heat from buildings and industrial facilities fits into this category [17]. For this, one requires a working fluid with a lower critical temperature than water and one that still has a high heat transfer coefficient during the low temperature rejection leg of the cycle. Supercritical carbon dioxide (SFCD) meets these requirements and has additional attractive characteristics which we now summarize:

1. SFCD has the potential to absorb and release heat at lower temperatures (approximately 373-300K) than water in cyclic power systems leading to the potential for enhanced waste heat recovery from processes.

2. The high density of SFCD (approximately 50 percent of liquid water density) implies that volumetric working fluid flow rates in industrial scale processes will not be prohibitive.

3. The high heat capacity of SFCD, which asymptotically approaches infinity at the critical point [18], indicates that heat transfer equipment sizes would be manageable if the rejection temperature is maintained near the working fluid’s critical temperature.

4. Carbon dioxide is widely available, relatively inexpensive, and non-toxic. It’s critical pressure (≈ 73 bar) is high, but well within the equipment design range in steam plants in which pressures in excess of 200 bar are often found [19].

We now illustrate how SFCD can be thermodynamically integrated into chemical processes for recovering waste heat from low temperature streams that would otherwise need to reject heat to an external coolant system.

II. THERMODYNAMIC APPROACH

2.1 Potential Work Available

^{1,2}University of Rochester Chemical Engineering Department

To test the self consistency of the computational code we developed, we first evaluated the theoretical work available from the cycle by numerical integration of the area within the cycle on a PV-Carnot cycle diagram and compared it to the work from the standard Carnot efficiency equation [2]. We used the Van der Waals (VDW) equation of state for our calculations, but any suitable equation of state can be used that satisfies the critical point stability criteria that lead to the flatness (point of inflection) of isotherms in the critical region [18]. From the Van der Waals equation, with reference to Figure 1, the heat input into the cycle is given by:

$$Q_H = \int_{V_1}^{V_B} \frac{RT_H}{V-b} dV = RT_H \ln\left(\frac{V_B - b}{V_1 - b}\right) \quad (1)$$

with the Carnot work:

$$W = Q_H \left(1 - \frac{T_C}{T_H}\right) \quad (2)$$

where T_H is the upper isotherm, T_C is the lower isotherm, V_B is the end volume on the upper isotherm, V_1 is the starting volume of the upper isotherm, and b can be calculated by the usual VDW equation. For the example illustrated in Figure 1 of a Carnot cycle running between 60°C to 31.03°C using a compression ratio of 2, the agreement between the analytic and numerical integration values for the available work was excellent.

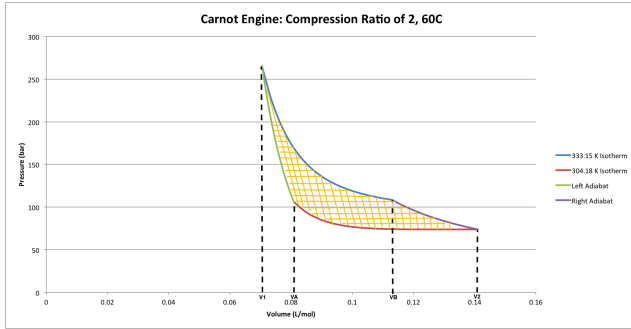


Fig. 1. Maximum Work of Carnot Cycle

2.2 Calculating Engine Size and Frequency

The computational code takes in the desired temperatures, compression ratio, and starting volume as inputs, then calculates the maximum theoretical work that the engine can output. In order to integrate this engine into the process network, it must be scaled in size to obtain the same power as the cooler it is to replace. By inputting the desired frequency (Hz) of the engine into the program, a conversion between work and power can be made, and the size of the engine determined. The units of power calculated from the program will be kW/mol, thus simple division of the cooler power by the generated power will yield the number of moles of supercritical CO₂ the engine is required to contain. An alternative calculation can be done with the program, inputting a specified engine size and receiving a required frequency to run it at. This calculation is more practical for industries that already have an engine and would like

to figure out how to integrate it into their process in order to utilize their waste heat. However, temperature and pressure limitations on power generation are factors that influence Carnot cycles and have to be accounted for [20].

III. RESULTS AND DISCUSSION

3.1 Replacing Cooler with Carnot Engine

Our analysis uses data from a flowsheet where stream matching according to the well-established Pinch Design method [21] led to a highly integrated heat exchange network structure shown in Figure 2. Our objective is to replace the 56.35 kW cooler in the network with a Carnot engine using SFCO₂ as a working fluid. This cooler functions to bring a stream with a heat capacity of 3.26 kW/°C down to a temperature of 80°C from 129°C. The waste heat can be thought of as the upper isotherm of the cycle fed into the engine, which does work and releases the heat to a coolant stream of supercritical CO₂ at 31.03°C. Since the desired temperature of the process stream is greater than 60°C, the entire heat load of the cooler can be captured if considering the self imposed 60°C limit. For practical purposes, it was assumed that 60°C was the lowest temperature to be fed into the Carnot cycle to maintain nontrivial Carnot efficiencies. Thus, instead of wasting the low grade heat, it will be used in its entirety to run a Carnot cycle.

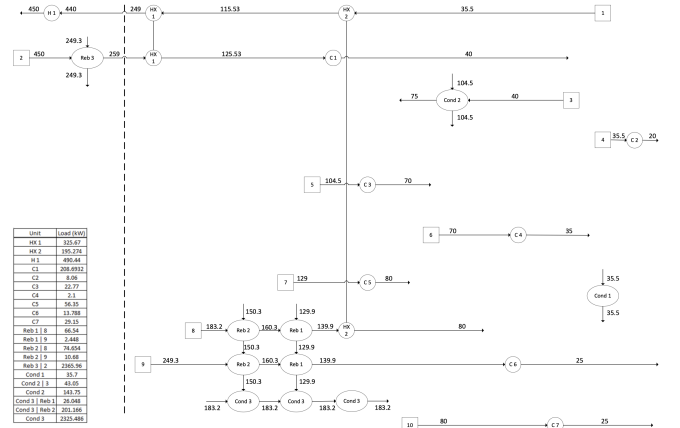


Fig. 2. Heat Exchange Network

The heat wasted, in terms of the power of the necessary cooler, was calculated using the following equations and information from the toluene process:

$$P_{cooler}(kW) = CP_{stream} \Delta T_{stream} \quad (3)$$

$$P_{cooler}(kW) = CP \Delta T \quad (4)$$

$$P_{cooler}(kW) = \left(1.15 \frac{kW}{C}\right) (129C - 80C) = 56.35kW \quad (5)$$

For initial calculations, the program was used to calculate the work available for an upper temperature of 353.15 K (80°C), lower temperature of 304.18K (31.03°C), an initial volume of 0.75V_C, and compression ratios of 1.5, 2, and 4. The value of 0.75V_C was arbitrarily chosen such that the

minimum compression and maximum expansion volumes of the cycle would straddle the critical volume of CO₂, which is around 0.094 L/mol, but not decrease so far as to increase the pressure significantly. Since the heat from the cycle is being rejected to CO₂ at its critical temperature, it is possible to obtain the relatively flat isotherm depicted Figures 3,4, and 5. From these compression ratios, the final expansion volume of the cycle could be calculated. Using the program, the two isotherms and two adiabatic curves for the process were calculated and plotted in Figures 3, 4, and 5.

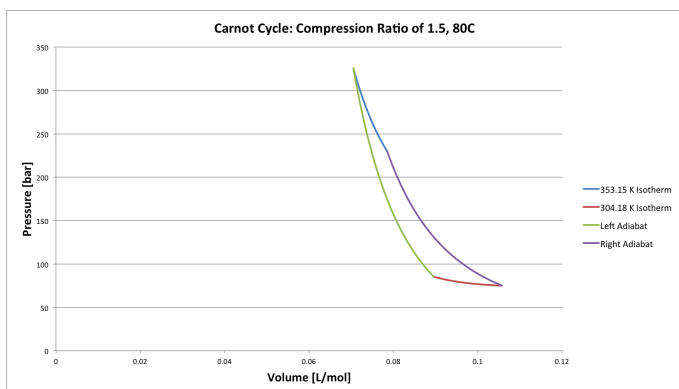


Fig. 3. Compression Ratio of 1.5

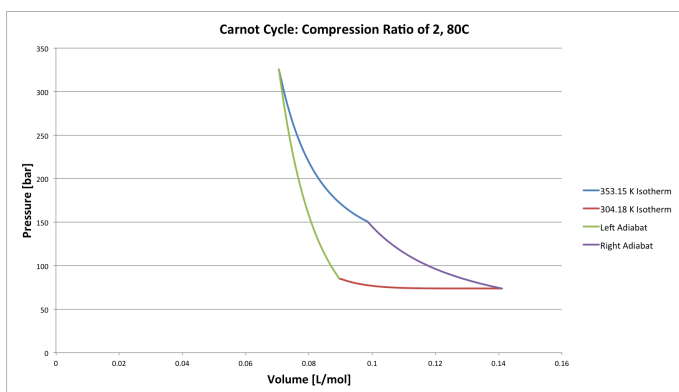


Fig. 4. Compression Ratio of 2

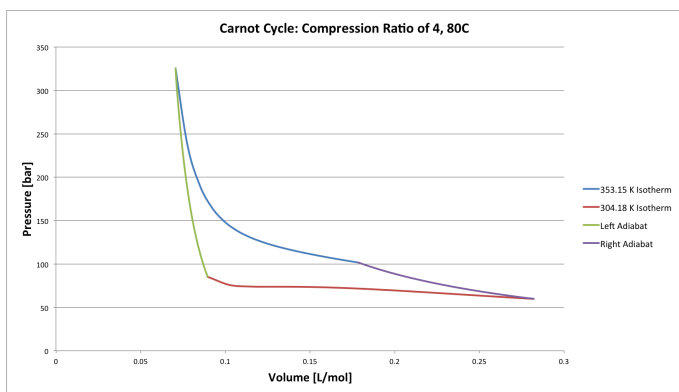


Fig. 5. Compression Ratio of 4

From the above figures, it is evident that as the compression ratio increases, so does the size of the engine, as indicated by the elongated cycle area and isotherms. To gain a better understanding of the impact of the compression ratio, the work available in each instance was found. These results are given in Table I.

Compression Ratio	Work [J/mol]
1.5	103.74
2	284.86
4	647.41

TABLE I
ANALYTICALLY CALCULATED WORK

At the same temperature and initial conditions, the larger the compression ratio, and thus the size of the engine, the greater the amount of available work. In fact, based on these trials, as the compression ratio doubled, the available work more than doubled. However, to implement these cycles into the network, the power of the engine must be calculated by designating a desired frequency of the engine.

For the purposes of this analysis, a standard value of 50 Hz was chosen as the frequency of the engine. Later, the program will be used to calculate the required frequency given a specified engine size. In general, the greater the operating frequency, the greater the power available. Larger engines usually have a compression ratio between 8 and 14, but the focus of this paper is smaller scale engines, ranging up to a compression ratio of 4 [22], that would be easy to integrate into any given chemical process. As seen in Figure 6, the larger the engine, the greater the amount of power available. It is important to note that these values are not yet scaled to the size needed for the given process and have units per mole working fluid.

$$\text{Power} = \text{Work} \times \text{Frequency (Hz)} \quad (6)$$

$$\text{Power} = 284.86 \times 50 = 14.34 \text{ kW per mol fluid} \quad (7)$$

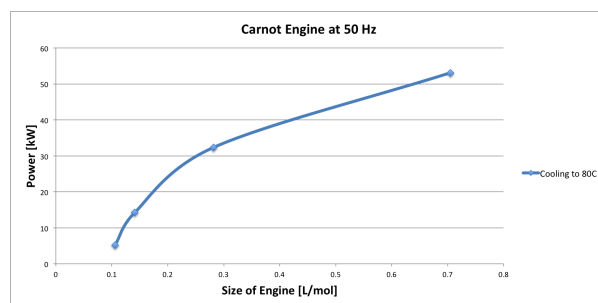


Fig. 6. Power vs. Size of Engine

To relate this Carnot cycle analysis to the process at hand, the engines must be scaled to size. The cooler on the analyzed process stream has a duty of 56.35 kW. Using the engine with a compression ratio of 2, the power produced is 14.34 kW per mole at a maximum volume of 0.141 L per mole of CO₂. To find the size of the engine, the power of

the pertinent cooler is divided by the power of the Carnot cycle to achieve a result of about 3.93 moles. The result is an engine size of 0.554 L.

$$\text{Moles Required} = \frac{\text{Cooler Duty}}{\text{Calculated Power}} \quad (8)$$

$$\text{Moles Required} = \frac{56.35 \text{ kW}}{14.34 \text{ kW/mol}} = 3.93 \text{ moles} \quad (9)$$

$$\text{Engine Size} = \text{Max Volume} \times \text{Moles} \quad (10)$$

$$\text{Engine Size} = 0.141 \text{ L/mol} \times 3.93 \text{ moles} = 0.554 \text{ L} \quad (11)$$

As a consistency check, the following calculations were done realizing that the power output should equal the power input multiplied by the Carnot efficiency.

$$P = \eta Q_{in} Hz \quad (12)$$

$$P = \left(1 - \frac{T_C}{T_H}\right) (Q_{calc}) (\text{moles}) (Hz) \quad (13)$$

$$56350 \text{ W} = \left(1 - \frac{304.18}{353.15}\right) (2054.26 \text{ J/mol}) (3.93 \text{ mol}) (50 \text{ s}^{-1}) \quad (14)$$

$$56350 \text{ W} \approx 55975 \text{ W} \quad (15)$$

This is about a 0.7%, showing the calculations are consistent.

Thus, it is possible to remove all wasted heat from the cooler with a 0.554 L engine that takes in this waste heat at 80°C and rejects it to a coolant stream of supercritical CO₂. This will result in a net generation of 56.35 kW of power that can be utilized elsewhere.

3.2 Decreasing the Wasted Heat of the Largest Cooler

Another interesting use of the Carnot cycle is decreasing a sizable cooler's heat load. In the given process, the heat exchanger network has a cooler releasing 208.69 kW as it decreases the temperature of a stream with heat capacity of 2.44 kW/°C from 125.53°C to 40°C. As a standard metric for this analysis, we considered that the Carnot cycle would take in a hot stream no cooler than 60°C. Thus, while not all of the wasted heat from the cooler could be utilized, it still is of benefit to examine the potential of re-purposing a decent portion of the otherwise waste heat from the cooler. For comparative analysis of the impact of upper isotherm temperatures, three different scenarios were proposed: feeding a hot stream at 60, 70, and 100°C into the Carnot cycle. From these analyses, the relationship between temperature and pressure within the Carnot cycle were made apparent.

Figures 7, 8, and 9 depict these respective Carnot cycles. As the temperature of the upper isotherm increased, the length of the isotherms decreased, thereby increasing the area enclosed by the cycle and raising pressure.

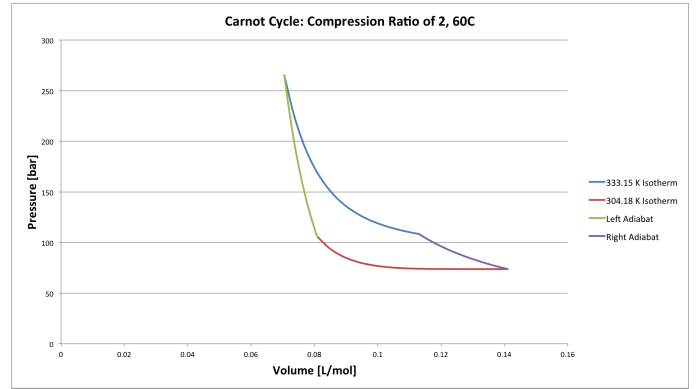


Fig. 7. 60°C Upper Isotherm

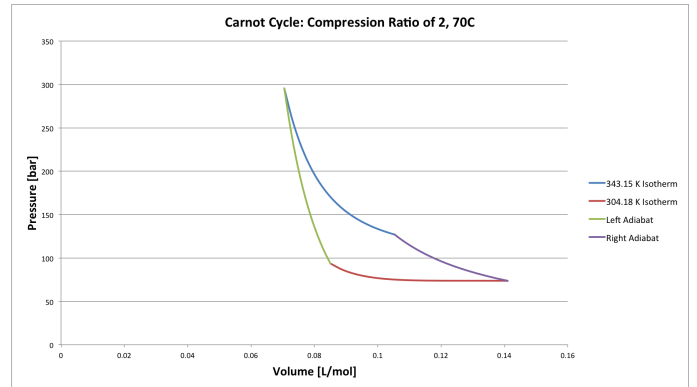


Fig. 8. 70°C Upper Isotherm

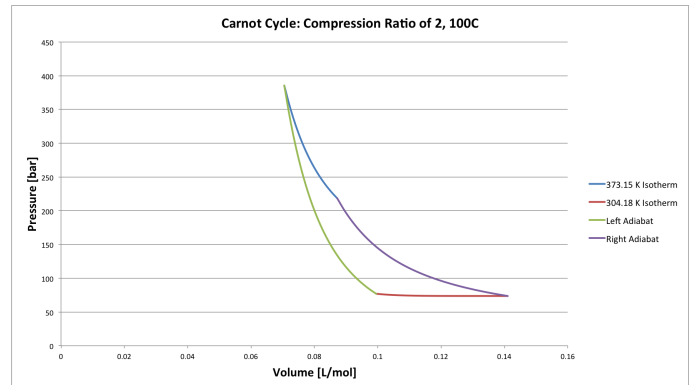


Fig. 9. 100°C Upper Isotherm

Using the program with a compression ratio of 2 and a frequency of 50 Hz, the following values for work, power, and maximum volume were obtained:

Upper Isotherm T [°C]	Work [J/mol]	Power [kW/mol]	Maximum Volume [L/mol]
60	224.14	11.21	0.141
70	264.00	13.20	0.141
100	270.56	13.53	0.141

TABLE II
ANALYTICALLY CALCULATED WORK AND POWER

By increasing the temperature of the input streams by 30°C, there is roughly a 21% increase in available power. However, as the difference in temperature between the isotherms increases, so does the pressure required for the compression of the engine. There is a significant increase in pressure required to go from 70°C to 100°C (≈30 bar) with only a small increase in available work (≈2%). Analogously, the efficiency of each process, according to the Carnot efficiency, only increases from 9%, to 11%, to 18% by increasing the temperature of the hot stream fed to the engine. While there is a large increase in efficiency by 100°C, the required pressure increase offsets its merits.

Upper Isotherm T [°C]	Engine Size [L]	Maximum Pressure [bar]
60	2.01	266
70	1.45	296
100	0.644	386

TABLE III
ENGINE SPECIFICATIONS

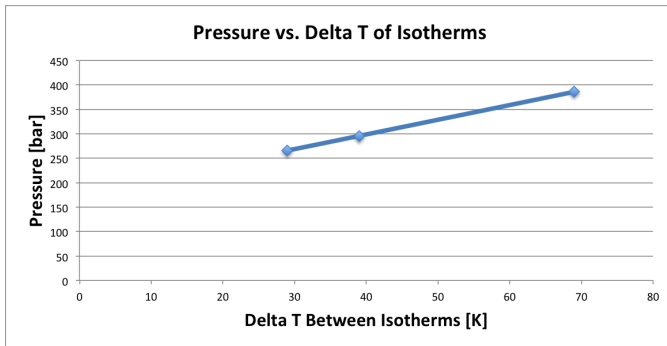


Fig. 10. Pressure vs. Delta T

We may conclude that the 2% increase in available work does not justify the need to design or obtain an engine that requires this increased pressure of almost 400 bar. Thus, it was decided to only further investigate a Carnot cycle running off of a 70°C upper isotherm.

Cooling the stream from 125.53°C to 70°C would release 135.49 kW. This was calculated by:

$$P_{released} = (2.44 \frac{kW}{C})(125.53C - 70C) = 135.49kW \quad (16)$$

To scale the Carnot cycle to this value, a factor of 10.26 moles is needed. This results in a final engine volume of 1.45 L and the desired output of 135.49 kW. That said, since 70°C was used as the input, there still must be a cooler present on the stream to decrease the temperature to the desired final value of 40°C. This will require a cooler that will reject 73.2 kW of low grade waste heat. This is still a 65% reduction in waste heat from this cooler.

$$P_{cooler} = (2.44 \frac{kW}{C})(70C - 40C) = 73.2kW \quad (17)$$

3.3 Calculating Required Frequency from Engine Size and Desired Power Output

Rather than analyzing the system to determine what size engine is needed, it may be more practical to fix the size of the engine and determine the frequency, or Hz, required. By fixing the isotherm temperatures, compression ratio, size of the engine, and the power output desired, the program was modified to calculate the required engine frequency. Using the same example as above (135.49 kW, compression ratio of 2, 70°C upper isotherm), the results in Table IV were obtained:

Engine Size [L]	Hz [s ⁻¹]
0.25	289.7
0.5	144.9
1	72.4
1.5	48.3
2	36.2
4	18.1
6	12.05

TABLE IV
FREQUENCY REQUIREMENT FOR GIVEN ENGINE SIZE

As the engine size increases, the frequency required decreases.

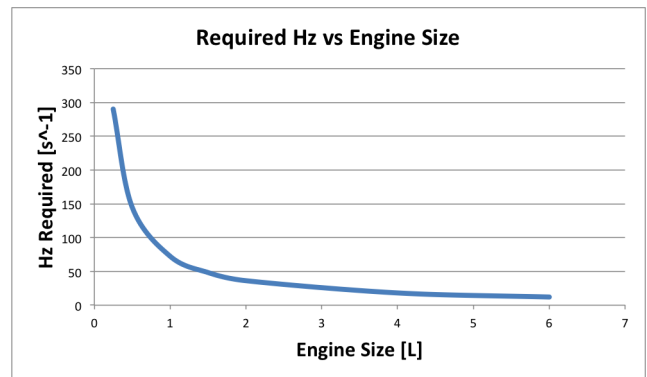


Fig. 11. Hz Requirement vs. Engine Size

While the above data only depicts the specific scenario outlined in this section, the same ideas can be applied to any circumstance where the isotherms, compression ratio, and desired power are known, as well as the size of the engine that is available.

3.4 Economic Benefits of Implementing Carnot Cycles to Capture Waste Heat

As illustrated using these two primary examples, there is significant potential to recover waste heat from a large industrial process and convert it into a usable form through a Carnot cycle with supercritical CO₂ as the working fluid. In the examples, even when the minimum temperature of the hot stream entering the cycle was constrained, a large portion of rejected waste heat could be captured with relatively small engine sizes. This generated power could be used to drive numerous aspects of an industrial plant, including furnaces, heat pumps, blowers, air conditioners, and compressors. Typical power needs, including start up values, are listed below in Table V.

Appliance	Power [W]
Lightbulb	60
Electric Water Heater	4,000
Sump Pump	4,000
Air Conditioner	4,500
Air Compressor	10,000
Furnace + Blower	15,000-20,000

TABLE V
POWER REQUIREMENTS FOR APPLIANCES [23]

Specifically addressing the example shown above, by implementing a Carnot cycle and engine into the process of interest, there is a maximum of 135.49 kW made available from decreasing the heat load of the largest cooler. By simply utilizing a 1.45 L engine on this one process stream provides 135.49 kW, 24 hours a day for 300 days, amounting to a savings of 975,528 kWh. This translates to thousands of dollars in energy savings for the plant per year. Various energy saving calculations are tabulated in Table VI below, illustrating the yearly cost savings from the implementation of this Carnot cycle on only one stream in this process.

Electricity Source	Price	Cost Savings per Year [\$]
NY State Industrial Average	\$.0612/kWh	59,702
National Average	\$0.0724/kWh	70,628
Conventional Coal	\$98.7/MWh	96,285
Biomass	\$95.3/MWh	92,968
Onshore Wind	\$48/MWh	46,825
Solar Thermal	\$126.6/MWh	123,502

TABLE VI
ENERGY SAVINGS[24] [25]

IV. CONCLUSION

We theoretically investigated the integration of a Carnot engine, using SFCD as the working fluid, to potentially recover low temperature waste heat from a realistic industrial chemical process. The use of SFCD is fundamentally key to the process concept given the low critical temperature of carbon dioxide and the high heat transfer coefficients available in the fluid's critical region. The program we developed calculates the engine size and/or frequency required to

utilize waste heat on the same scale it is being generated as waste heat by the process. The impacts of compression ratio, pressure, and isotherm temperatures on power production and engine size were analyzed and showed the significant potential for using the approach on large scale processes. Finally, we are currently planning to build a prototype engine on the scale of the one designed here for use in future experimental work.

ACKNOWLEDGMENT

Chemical Engineering Department, University of Rochester

REFERENCES

- [1] J.T. Banchemo B.D. Smith (Ed.) R.J. Hengstebeck. 'Disproportionation of toluene'. 1969.
- [2] E.H. Chimowitz Y.He, G.L. Shebert. 'An algorithm for waste heat recovery from chemical processes'. *Computers and Chemical Engineering*, 73, 17, 2015.
- [3] Smith J. C. Harriott P. McCabe, W. L. 'Unit operations of chemical engineering.' 5th edn. *McGraw-Hill*, 1993.
- [4] G. Lorentzen. 'Revival of carbon-dioxide as a refrigerant'. *Int J Refrig* 17, 292-301, 1994.
- [5] D. Q. Kern. 'Process heat transfer.' international edn. McGraw-Hill, 1965.
- [6] King C. W. Webber M. E. Duncan I. J. Hardberger A. Stillwell, A. S. 'Energy-water nexus in texas'. *The University of Texas at Austin, Environmental Defense Fund*, 2009.
- [7] U.S. D.O.E. 'Energy demands on water resources: Report to congress on the interdependency of energy and water'. 2006.
- [8] P. Carles. 'Thermoacoustic waves near the vapor-liquid critical point'. *Phys. Fluids* 18, 126102-126109, 2006.
- [9] Chimowitz E.H. Carles, P. 'Materials and processes for efficient heat transfer through a near-critical fluid film'. Preliminary Patent Application filed, *University of Rochester, Rochester, N.Y.*, 2008.
- [10] Ugurtas B. Carles, P. 'The onset of free convection near the liquid-vapour critical point - part I: Stationary initial state'. *Physica D* 126, 69-82, 1999.
- [11] Zappoli B. Carles, P. 'The unexpected response of near-critical fluids to low-frequency vibrations'. *Phys Fluids* 7, 2905-2914, 1995.
- [12] S. H. Yoon. 'Heat transfer and pressure drop characteristics during the in-tube cooling process of carbon dioxide in the supercritical region'. *Int J Refrig* 26, 857-864, 2003.
- [13] Chen T. K. Li H. X. Yin, F. 'An investigation on heat transfer to supercritical water in inclined upward smooth tubes'. *Heat Transfer Eng* 27, 44-52, 2006.
- [14] Takano N. Oka Y. Koshizuka, S. 'Numerical-analysis of deterioration phenomena in heat-transfer to supercritical water'. *Int J Heat Mass Tran* 38, 3077-3084, 1995.
- [15] Mori H. Yoshida, S. 'Heat transfer to supercritical pressure fluids flowing in tubes'. *SCR-2000*, 72-78, 2000.
- [16] Dejoan A. Garrabos Y. Beysens D Nikolayev, V. S. 'Fast heat transfer calculations in supercritical fluids versus hydrodynamic approach'. *Phys Rev E* 67, 061202-061213, 2003.
- [17] H. Tijani. 'Thermoacoustic system for energy saving'. *Energy Research Center of the Netherlands*, 2009.
- [18] E. H. Chimowitz. 'Introduction to critical phenomena in fluids'. *Oxford University Press*, 2005.
- [19] Sesonke A. Glasstone, S. 'Nuclear reactor engineering'. *Chapman-Hall*, 1994.
- [20] E.H.Chimowitz S.Makuc. 'Supercritical CO2 Carnot engine for industrial waste heat recovery and utilization'. *12th European Conference in Chemical Engineering, Florence, Italy*, September 15-20, 2019.
- [21] I. C. Kemp. 'Pinch analysis and process integration.' 2nd edn. *Elsevier*, 2007.
- [22] Marcus Klein. 'A Specific Heat Ratio Model and Compression Ratio Estimation'. *Linkoping University*, 2004.
- [23] American Honda Motor Co. Inc. 'Wattage Estimation Guide'.
- [24] New York State Energy Research and Development Authority. 'Monthly Average Retail Price of Electricity - Industrial'. October 05, 2018.

[25] U.S. Energy Information Administration. 'Levelized Cost and Avoided Cost of New Generation Resources in the Annual Energy Outlook 2018'. March 2018.